

Electronic Supplementary Information

Photoacoustic ratiometric assessment of mitoxantrone release from theranostic ICG-conjugated mesoporous silica nanoparticles

Giuseppe Ferrauto,^{a†} Fabio Carniato,^{b†} Enza Di Gregorio,^a Mauro Botta,^b and Lorenzo Tei^{*b}

^a *Department of Science and Technological Innovation, Università del Piemonte Orientale, Viale T. Michel 11, 15121 Alessandria, Italy*

^b *Department of Molecular Biotechnology and Health Science, University of Turin, Via Nizza 52, 10126 Torino, Italy*

† these authors equally contributed to the work

List of content

1. Experimental section
 - 1.1 Chemicals and materials
 - 1.2 Synthesis of the organo-modified silica nanoparticles
 - 1.3 Characterization techniques
 - 1.4 Cells and animals
 - 1.5 Photoacoustic imaging
 - 1.6 Assessment of MTX release
2. Supplementary references
3. Supplementary Figures and schemes

1. Experimental section

1.1 Chemicals and materials

All chemicals were purchased from Sigma-Aldrich Co. LLC and used without further purification. Human Serum (Serorm) was purchased from Sera, Norway.

Cell media and supplements (RPMI, FBS, Glutamine, pen/strep, MycoAlert™ Mycoplasma Detection Kit) were purchased from Lonza Sales AG-EuroClone SpA, Milano (IT).

TS/a murine breast cancer cells were derived at the University of Torino from a spontaneous mammary adenocarcinoma which arose in a retired breeder BALB/c female.

Balb/c mice were purchased from Charles River Laboratories.

1.2 Synthesis of the organo-modified silica nanoparticles

NH₂-MSN: Mesoporous silica nanoparticles (MSN) were prepared by adopting the procedure reported in the literature.¹ The sample after calcination at 600°C for 3h in air flow, was activated under vacuum at 250 °C for 2 h in order to remove the physisorbed water. 780 mg for the dehydrated material were suspended in 100 mL of toluene under N₂ flow and 3-aminopropyltriethoxysilane (40 wt%, 312 mg) was added to the suspension. The mixture was heated at 50 °C and stirred for 20 h. The final material (NH₂-MSN) was filtered and washed with toluene and diethyl ether. Finally, NH₂-MSN was dried at 60°C for 2 h. The number of amino groups was quantified by elemental analysis (CHN) to be 1.25 mmol g⁻¹.

PEG-NH₂-MSN: 480 mg of NH₂-MSN were suspended in 15 mL of ultra-pure water and stirred for 15 min. In parallel, 167 mg of PEG₃₀₀₀COOH were dissolved in water (30 mL) in the presence of 69 mg of 1-ethyl-3-(3-dimethylaminopropyl)carbodiimide hydrochloride (EDC) and 140 mg of N-hydroxysulfosuccinimide (Sulfo-NHS). The solutions were mixed and stirred at room temperature for 4.5 h. The final material was filtered, washed with water and dried at 50°C for 4h. The PEG loading on the silica surface was quantified by CHN analysis as 0.021 mmol g⁻¹.

MTX-PEG-NH₂-MSN (MTX-MSN): 104 mg of PEG-NH₂-MSN and 15 mg of MTX were added to 10 mL of ultra-pure water and stirred at room temperature for 24h. The suspension was then centrifuged at 8500 rpm at 12°C for 4 min. The powder was separated by the liquid phase and dried at 75°C for 2h. MTX loading was quantified as 38.0 μmol g⁻¹ by the UV-Visible analysis of the drug remained in solution after centrifugation (Fig. S1).

ICG-PEG-NH₂-MSN (ICG-MSN): 100.2 mg of PEG-NH₂-MSN were suspended in 10 mL of DMF in the presence of 500 μL of Indocyanine green NHS active ester (ICG-NHS) solution (4.8 mg of ICG-NHS in 10 mL of DMF) in the dark. The suspension was stirred at room temperature for 4h and

ICG-MSNs were separated by centrifugation (4000 rpm for 4 min). The amount of ICG attached to the silica surface ($0.3 \mu\text{mol g}^{-1}$) was indirectly quantified via UV-Vis analysis by measuring the spectrum of the free dye in DMF solution (Fig. S1).

MTX-ICG-PEG-NH₂-MSN (MTX-ICG-MSN): 100 mg of ICG-MSN and 2.9 mg of mitoxantrone were mixed in 10 mL of methanol. The suspension was stirred at room temperature for 24h in the dark. The final powder was isolated by centrifugation at 4000 rpm for 4 min. MTX and ICG loading in MTX-ICG-MSN was assessed by measuring the amount of free drug and dye in the washing media with UV-visible spectroscopy. The UV-Visible bands selected for the analysis are at 609 and 780 nm, typical of MTX and ICG, respectively (Fig. S1). The amount of MTX and ICG was $22.6 \mu\text{mol g}^{-1}$ and $0.3 \mu\text{mol g}^{-1}$, respectively.

1.3 Characterization techniques

- HRTEM micrographs were obtained with a JEOL 3010 High Resolution Transmission Electron Microscope operating at 300 kV. The sample was dispersed and sonicated in isopropanol, and few drops of the suspension were deposited on the carbon-coated grids.
- X-ray diffraction profiles were collected on a ARL XTRA48 diffractometer using CuK α radiation of $\lambda=1.54062 \text{ \AA}$.
- Infrared spectra were obtained under vacuum conditions in the range $4000\text{--}400 \text{ cm}^{-1}$ with a resolution of 4 cm^{-1} , using a Bruker Equinox 55 spectrometer.
- N₂ physisorption curves were obtained at -196°C in the relative pressure range from 1×10^{-6} to 1 P/P_0 with a Quantachrome Autosorb 1MP/TCD instrument. The samples were out gassed at 100°C for 3 h. The specific surface area was calculated by using the BET equation, in the relative pressure range from 0.01 to 0.1 P/P_0 . Pores volume and diameter determined by the Barret–Joyner–Halenda (BJH) approach.
- UV-visible spectra were collected by using a Perkin Elmer Lambda 900 spectrometer equipped with a diffuse reflectance sphere accessory.
- Photoluminescence spectra were measured with a Horiba Jobin-Yvon Model IBH FL-322 Fluorolog 3 spectrometer equipped with a 450 W xenon arc lamp, double-grating excitation and emission monochromators (2.1 nm/mm dispersion; 1200 grooves/mm), and a Hamamatsu Model R928 photomultiplier tube. Emission spectra were corrected for source intensity (lamp and grating) and emission spectral response (detector and grating) by standard correction curves.

- Dynamic light scattering (DLS) analysis was realized on a suspension of the particles in aqueous solution by using a Zetasizer NanoZS instrument, Malvern (UK) equipped with a He-Ne laser ($\lambda=633$ nm). Surface ζ -potential was evaluated in water at 25°C by using the same instrument.

1.4 Cells and animals

The metastasizing mouse cell line (TS/A) derived from a mammary adenocarcinoma that arose spontaneously in a BALB/c female mouse was generously provided by Prof. Federica Cavallo, Department of Molecular Biotechnologies and health sciences, University of Turin, Italy.² They were grown in RPMI (Roswell Park Memorial Institute)¹⁰⁶⁴ medium supplemented with 10% heat-inactivated fetal bovine serum (FBS), 2 mM glutamine, 100 U/ml penicillin and 100 μ g/ml streptomycin. Cells were seeded in 75-cm² flasks at density of *ca.* 2×10^4 cells/cm² in a humidified 5% CO₂ incubator at 37 °C. At confluence, they were detached by adding 1 mL of Trypsin-EDTA solution (0.25 % (w/v) Trypsin- 0.53 mM EDTA). Cells were negative for mycoplasma as tested by using MycoAlert™ Mycoplasma Detection Kit. All cell media and supplements were purchased from Lonza Sales AG-EuroClone SpA, Milano (IT).

For the *in vivo* experiments, Balb/c mice were used (Charles River Laboratories, Calco, Italy). Mice were kept in standard housing with standard rodent chow and water available *ad libitum*, and a 12 h light/dark cycle.

Experiments were performed according to the Amsterdam Protocol on Animal Protection and in conformity with institutional guidelines in compliance with national laws (D.L.vo 116/92, D.L.vo 26/2014 and following additions) and international laws and policies (2010/63/EU, EEC Council Directive 86/609, OJL 358, Dec 1987, NIH Guide for the Care and Use of Laboratory Animals, U.S. National Research Council, 1996). This study was carried out in the framework of a protocol approved by Italian Ministry of Health (n. 229/2016-PR).

For the tumour model preparation, *ca.* 5×10^5 TS/A breast cancer cells were suspended in 0.1 mL of PBS and subcutaneously injected in the leg of 8-weeks male mice (N=3, a low number in agreement with 3Rs principles for the use of animals, by considering that only a proof of concept of the *in vivo* feasibility of the proposed method was required).

For the photoacoustic experiments, mice were anesthetized by intramuscular injection of tiletamine/zolazepam (Zoletil 100; Virbac, Milan, Italy) 20 mg/kg plus xylazine (Rompun; Bayer, Milan, Italy) 5 mg/kg by using a 27-G syringe.

A permanent vein access was obtained by inserting a PE10 catheter into the tail vein (27-G needle).

Animals were monitored weekly for changes in tumour size by caliper. PAI was performed 3 weeks after tumour cells implantation when the mean tumour volume is *ca.* 700 mm³.

Mice were sacrificed after PAI experiments by cervical dislocation.

1.5 Photoacoustic imaging

All US and PA images were acquired on a VisualSonics Vevo 2100 LAZR Imaging Station (VisualSonics, Inc., Toronto, Canada) equipped with a LZ250 transducer operating at 21 MHz. The *in vitro* PAI characterization of MSNs was carried out by preparing a phantom constituted by thin-layer plastic tubes surrounded by 1% agarose gel. Specimens to be analysed were loaded inside capillaries by using a syringe.

An US gel was applied over the region of interest before image acquisition. As reference image, grey scale B-mode US images at high resolution were acquired. This was carried out by using a high-frequency ultrasound probe (MS550D, VisualSonics, Canada, broadband frequency: 22 MHz - 55MHz, image axial resolution: 40 μ m) operating at 40 MHz. For PA imaging a 21 MHz frequency probe was used, provided with a laser tuneable in the 680-970 nm range. The laser energy was continuously monitored and eventually adjusted through laser recalibration and optimization, in order to acquire PA images with the same energy. PA spectra were acquired investigating the region 680-970 nm, with 2 nm steps (persistence=4). PA images of ICG were acquired by setting wavelength at 810nm (persistence=4). PA images of MTX were acquired by setting wavelength at 700 nm (persistence=4).

For *in vivo* experiments, 3 mice bearing subcutaneous TS/A cells were used. Mice were anesthetized by intramuscular injection of tiletamine/zolazepam (Zoletil 100; Virbac, Milan, Italy) 20 mg/kg plus xylazine (Rompun; Bayer, Milan, Italy) 5 mg/kg by using a 27-G syringe. Hairs were removed over the tumour area using a depilatory cream.

A permanent vein access was obtained by inserting a PE10 catheter into the tail vein (27-G needle) for the following *i.v.* injection of MSNs. An US gel was applied on the region of interest before image acquisition. US and PA images were acquired as above reported. PAI spectra and PA images of tumour region were acquired before and after (t=0 and t=30 min) the slow *i.v.* injection of 3mg of MSNs (15 mg/mL, 0.2mL, single dose). All PA images were co-registered with grey scale B-mode-US imaging. ROIs were manually drawn, and PA signal intensity measured.

1.6 Assessment of MTX release

The release of MTX from MTX-MSNs and MTX-ICG-MSNs was assessed by using PAI and UV-Visible spectroscopy. To monitor drug release via UV-Vis, 5.0 mg of sample was

dispersed in 5.0 mL of phosphate-buffered saline (PBS) at 25°C. MTX remained in solution over the time was analysed by UV-Visible spectroscopy, monitoring the absorbance of the band at 609 nm.

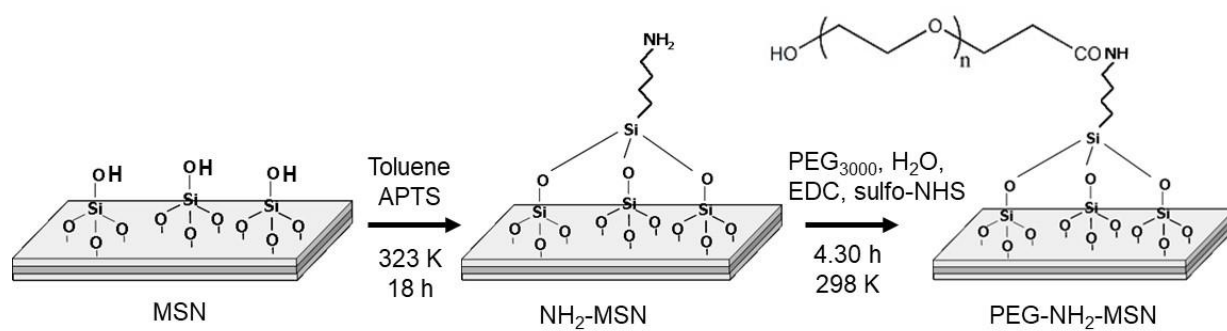
In case of PAI detection of drug release, first, the amount of MTX remained in MSNs samples was monitored. PAI signal of MTX-ICG-MSNs was acquired at t=0 and t=24h post dissolving MSNs in 0.5 mL of water or Human Serum (Seronom purchased from Sera, Norway). Briefly, 8 mg/mL of MTX-ICG-MSNs were dissolved in water or in serum and PA images (at 700nm and 810 nm) were acquired immediately after the dissolution (t=0). Then, MSNs were left at 25°C for 24h to allow drug release, centrifuged and supernatant replaced by fresh one, to re-suspend the MSNs. PA image of samples were re-acquired to quantify the amount of MTX maintained in MTX-MSNs or MTX-ICG-MSNs.

In a second approach, the amount of MTX in the supernatant (*i.e.* released by MSNs) was measured. In particular, MTX-ICG-MSNs and MTX-MSNs were dissolved in 0.5 mL of water or human serum at the final MSNs concentration of 8 mg/mL and then they were left at 25°C. At variable time points (t=5, 15, 30, 45 min, 1h,3h, 7h, 24h and 48h) samples were centrifuged at 3000 rpm and 0.3 mL of supernatant was collected for each sample and substituted with fresh one. The collected supernatants were analysed by using PAI (at 700nm and 810 nm) to quantify the amount of MTX released from MTX-MSNs and MTX-ICG-MSNs.

2. Supplementary references

1. K. Suzuki, K. Ikari, H. Imai, *J. Am. Chem. Soc.* 2004, **126**, 462–463
2. P. Nanni, C. De Giovanni, P.L. Lollini, G. Nicoletti, G. Prodi. *Clin. Exp. Metastasis*, 1983, **1**, 373-380.

3. Supplementary Figures and schemes



Scheme S1. Schematic view of the synthesis of NH₂-MSN and PEG-NH₂-MSN samples.

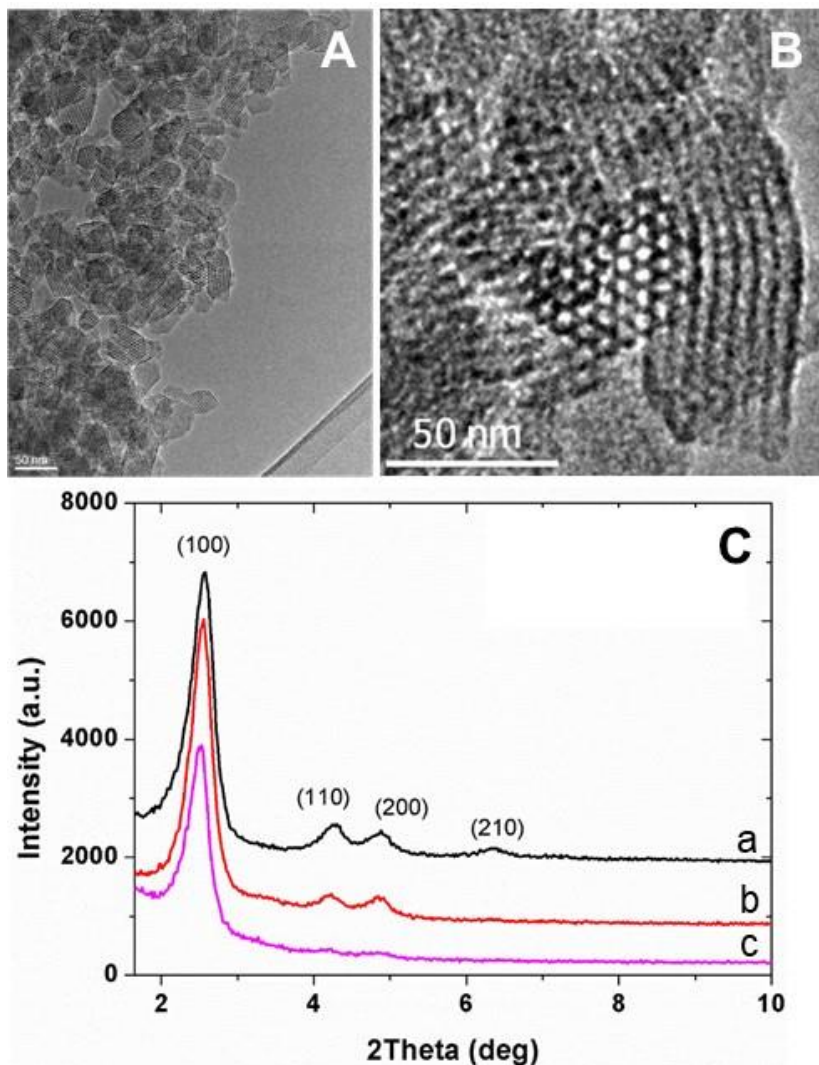


Figure S1. HRTEM micrographs at low (A) and high magnifications (B) of MSN nanoparticles; C) X-ray patterns of MSN (a), NH₂-MSN (b) and PEG-NH₂-MSN (c). The particles are characterized by appreciable crystallinity with a structure comparable to the traditional MCM-41. The diffraction peaks at 2.4, 4.0 and 4.8 2 θ are assigned to the (100), (110) and (200) planes, respectively, typical of porous silica with a hexagonal pore array. The X-ray profiles of NH₂-MSN and pegylated sample (PEG-NH₂-MSN) show a gradual decrease of the peaks intensity respect to the pristine MSN. This is mainly due to the modification of the scattering properties of the solids, promoted by the presence of some organic moieties on the silica surface. However, the signal at low angles appears narrow, proving that the structural order was preserved after NH₂ anchoring and reaction with PEG molecules.

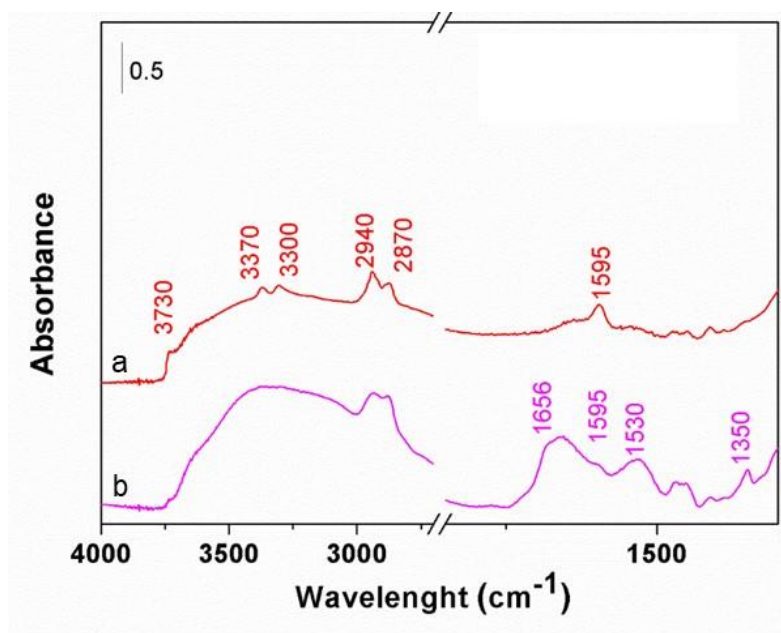


Figure S2. FT-IR spectra in vacuum at 298 K of NH₂-MSN (a) and PEG-NH₂-MSN (b). Along with the peak at 3700 cm⁻¹ assigned to the presence of residual isolated silanol groups, the spectrum of NH₂-MSN shows bands at 3370 and 3300 cm⁻¹ and 1595 cm⁻¹ assigned to the asymmetric and symmetric stretching and bending modes of the amino groups, respectively. Peaks at 2940 and 2870 cm⁻¹ are also observed and attributed to the stretching modes of -CH₂ of aminopropyl fractions. The reaction of the NH₂ with PEG molecules promoted a modification of the IR spectrum. Indeed, the peaks previously assigned to the stretching vibrations of NH₂ are less intense and two new bands at 1656 and 1530 cm⁻¹ are correlated to the stretching and bending of the CO and NH of the amide groups, respectively, formed in the anchoring reaction.

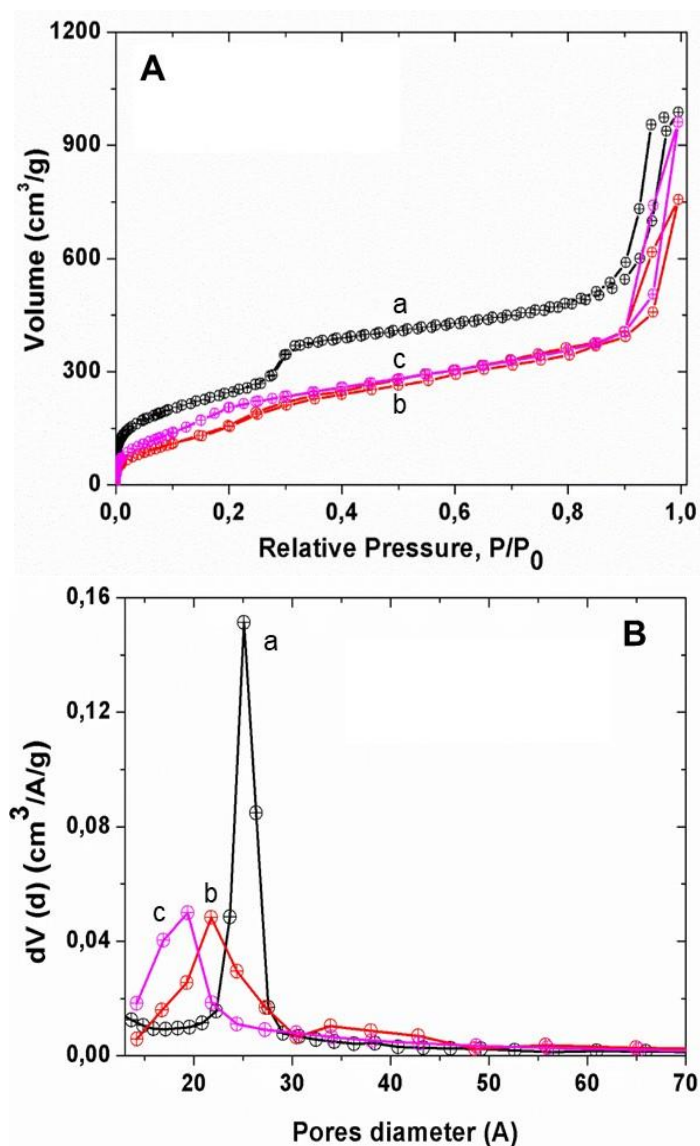


Figure S3. A) N₂ adsorption/desorption isotherms at -196°C of MSN (a), NH₂-MSN (b) and PEG-NH₂-MSN (c); B) Pore-size distribution obtained by the BJH method at -196°C for MSN (a), NH₂-MSN (b) and PEG-NH₂-MSN (c). All the materials show isotherms of type IV, according to the IUPAC classification with a specific surface area of 890 m² g⁻¹ for MSN and 708 and 578 m² g⁻¹ for NH₂-MSN and PEG-NH₂-MSN, respectively. The analysis of the pores diameter shows a decrease from 2.5 nm for MSNs to 2.18 and 1.94 nm after functionalization with NH₂ and PEG molecules

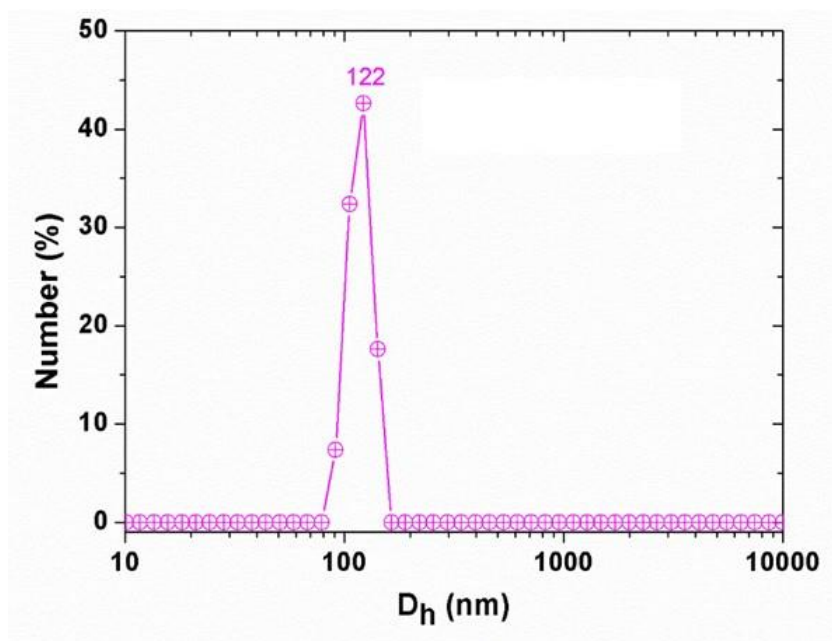


Figure S4. Particles size distribution in water of PEG-NH₂-MSN sample at neutral pH and 298 K.

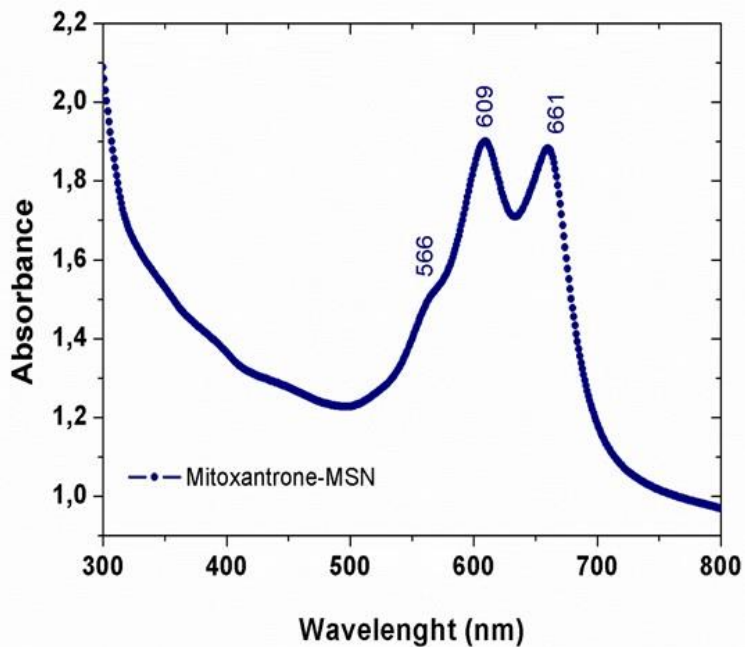


Figure S5. UV-Visible spectrum of MTX-MSN in aqueous solution (pH 7 and 298 K).

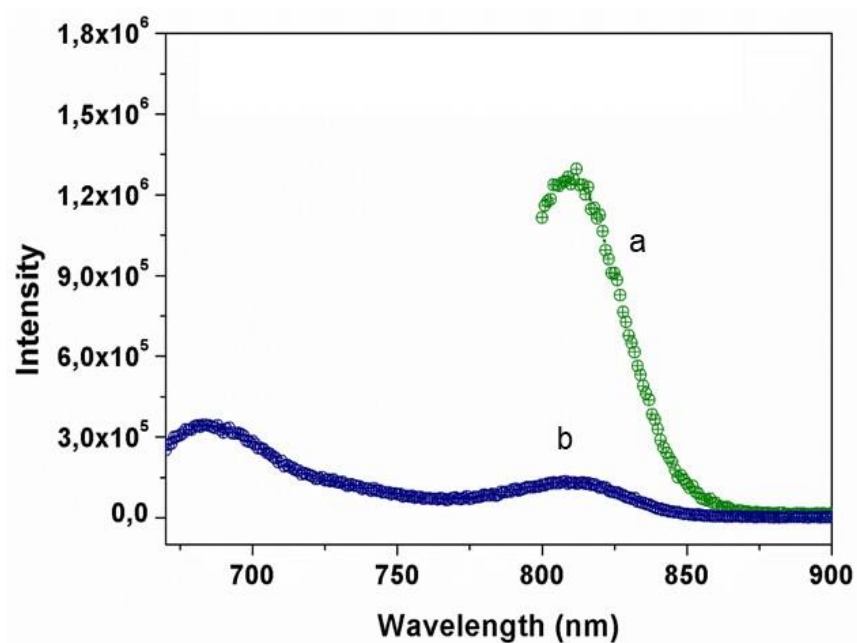


Figure S6. Photoluminescence spectra of MTX-ICG-MSN under excitation at 790 nm (a) and 660 nm (b) in water at 298 K. [ICG] = 0.15 μ M.

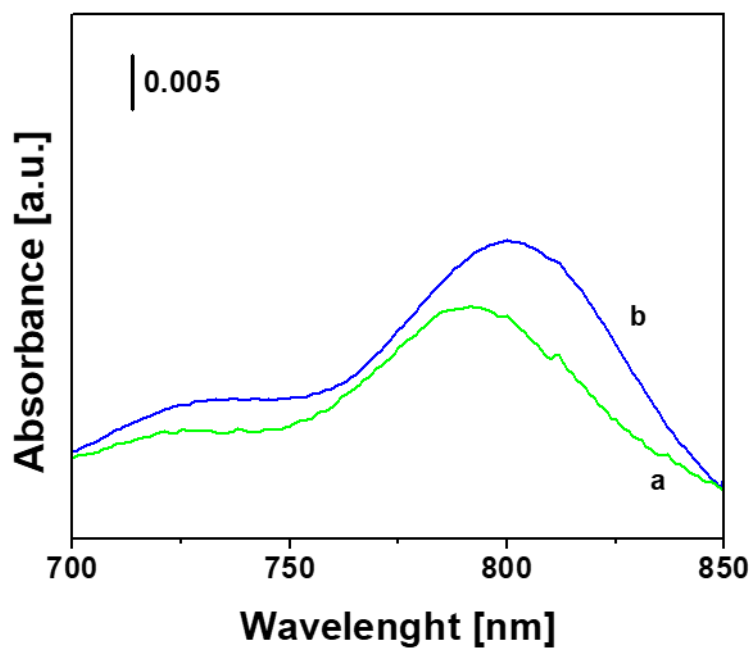


Figure S7. UV-Visible spectrum of ICG-MSN in water before (a) and after dispersion (b) in Seronorm™ at 298 K. The test in biological fluid was realized by dispersing 6 mg of ICG-MSNs in 3 mL of a Seronorm™ solution and monitoring the UV-Vis absorbance of the dye.

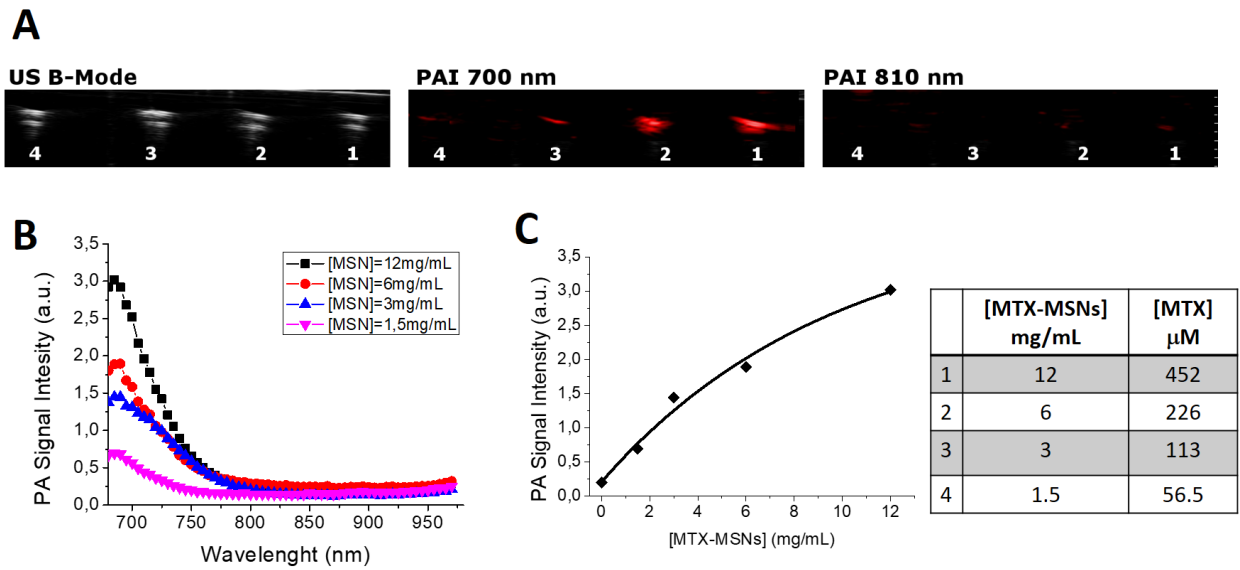


Figure S8. Representative US-B-Mode image (*left*), PA image at 700 nm (*middle*) and PA image at 810 nm (*right*) of a phantom containing plastic tubes filled with MTX-MSNs at different concentration (1= 12mg/mL, 2=6mg/mL, 3=3mg/mL and 4=1.5mg/mL); (B) PA spectra of solutions at different concentration of MTX-MSNs; (C) PA signal intensity vs. [MTX-MSNs]. Table reports correlation between MTX-MSNs concentration (mg/mL) and MTX concentration (μ M).

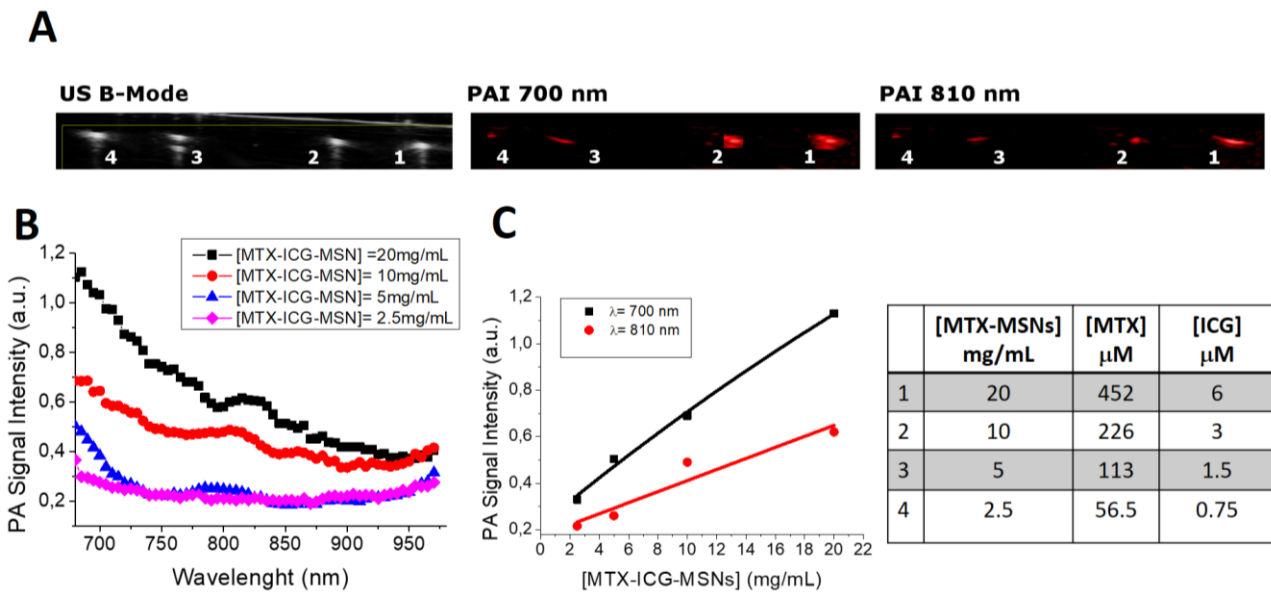


Figure S9. Representative US-B-Mode image (*left*), PA image at 700 nm (*middle*) and PA image at 810 nm (*right*) of a phantom containing plastic tubes filled with MTX-ICG-MSNs at different concentration (1= 20mg/mL, 2=10mg/mL, 3=5mg/mL and 4=2.5mg/mL); (B) PA spectra of solutions at different concentration of MTX-ICG-MSNs; (C) PA signal intensity vs. [MTX-ICG-MSNs]. Table reports correlation between MTX-ICG-MSNs concentration (mg/mL) and MTX concentration (μ M) and ICG concentration (μ M).

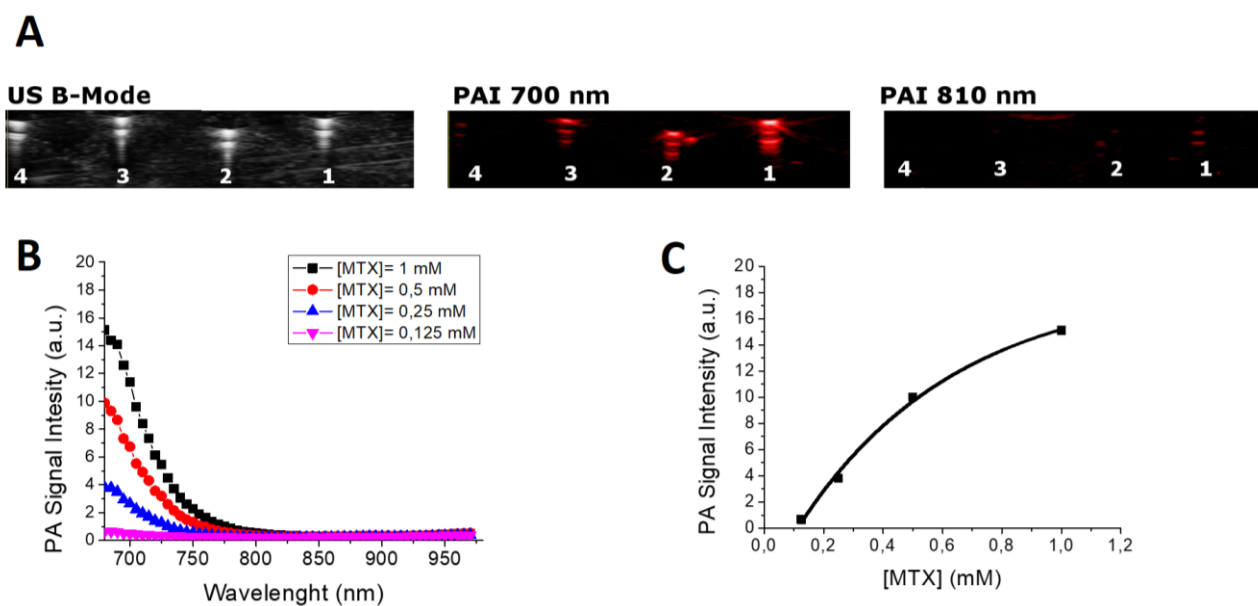


Figure S10. (A) Representative US-B-Mode image (*left*), PA image at 700 nm (*middle*) and PA image at 810 nm (*right*) of a phantom containing plastic tubes filled with MTX water solutions at different concentration (1= 1mM, 2=0.5mM, 3=0.25mM and 4=0.125mM); (B) PA spectra of solutions at different concentration of MTX; (C) PA signal intensity vs. [MTX].

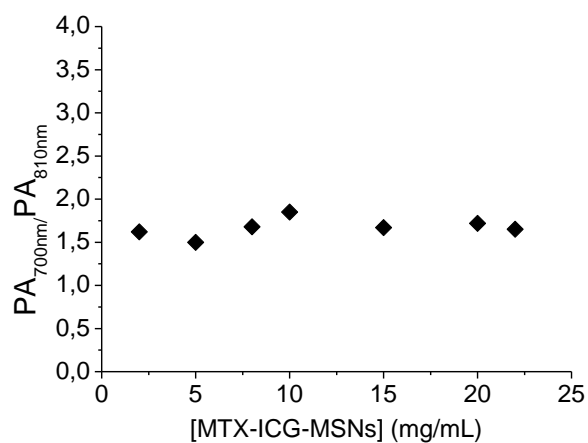


Figure S11 PA_{700nm}/PA_{810nm} assessed at variable dilution of MTX-ICG-MSNs. The man value was 1.67± 0.17



Figure S12 (A) Representative PA image at 700 nm of supernatants of washing solutions (water) of MTX-MSNs at variable times (1: 5min, 2:15min, 3:30min, 4:45min, 5:1h, 6:3h, 7:7h, 8: 24h and 9: 48h); (B) Representative PA image at 700 nm of supernatants of washing solutions (water) of MTX-ICG-MSNs at variable times (1: 5min, 2:15min, 3:30min, 4:45min, 5:1h, 6:3h, 7:7h, 8: 24h and 9: 48h).

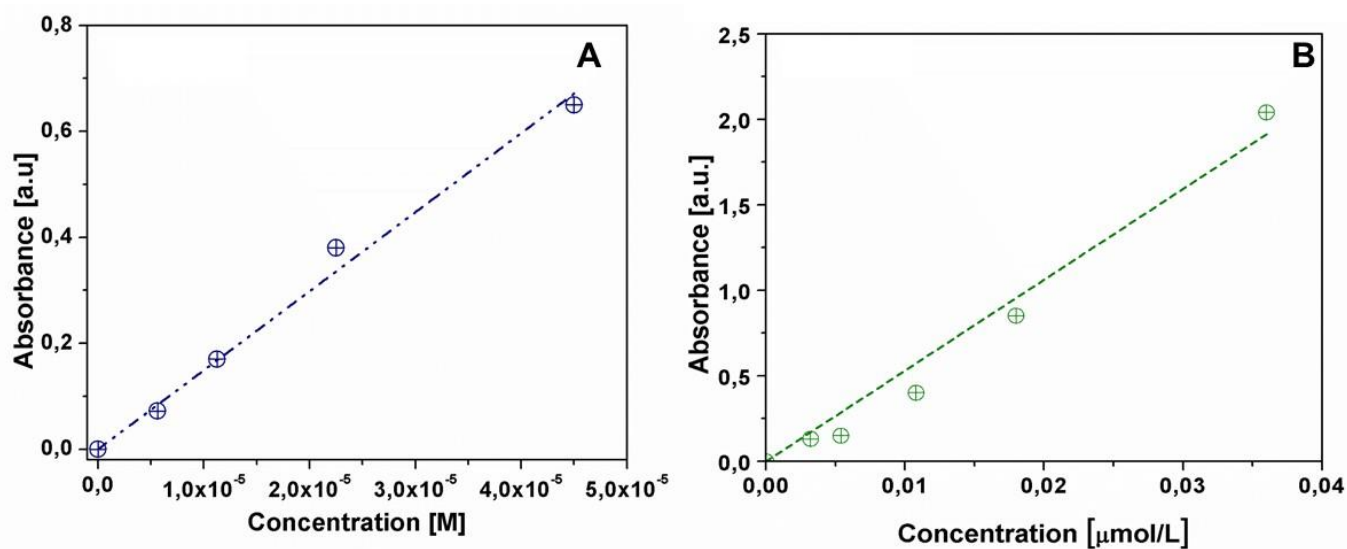


Figure S13. Calibration curves obtained by UV-Visible spectra ($\lambda = 609$ nm for mitoxantrone and 790 nm for ICG) of mitoxantrone in water (A) and ICG in DMF solution (B).